Clinical & Translational Immunology

Australian and New Zealand Society for Immunology Inc.

Clinical & Translational Immunology 2020; e1200. doi: 10.1002/cti2.1200
www.wileyonlinelibrary.com/journal/cti

ORIGINAL ARTICLE

Ex vivo enrichment of PRAME antigen-specific T cells for adoptive immunotherapy using CD137 activation marker selection

Koon H Lee[1,2], Kavitha Gowrishankar[1], Janine Street[1], Helen M McGuire[2,3,4,5], Fabio Luciani[6], Brendan Hughes[6], Mandeep Singh[7,8], Leighton E Clancy[1,9], David J Gottlieb[1,2,10], Kenneth P Micklethwaite[1,2,10] & Emily Blyth[1,2,10]

[1]Westmead Institute for Medical Research, Westmead, NSW, Australia
[2]Faculty of Medicine and Health, Sydney Medical School, Sydney, NSW, Australia
[3]Ramaciotti Facility for Human Systems Biology, The University of Sydney, Sydney, NSW, Australia
[4]Charles Perkins Centre, University of Sydney, Sydney, NSW, Australia
[5]Discipline of Pathology, Faculty of Medicine and Health, The University of Sydney, Camperdown, NSW, Australia
[6]The Kirby Institute, University of New South Wales, Darlinghurst, NSW, Australia
[7]The Garvan Institute of Medical Research, Darlinghurst, NSW, Australia
[8]St Vincent's Clinical School, Faculty of Medicine, UNSW Sydney, Sydney, NSW, Australia
[9]Sydney Cellular Therapies Laboratory, Westmead, NSW, Australia
[10]Department of Haematology, Westmead Hospital, Westmead, NSW, Australia

Correspondence
E Blyth, Faculty of Medicine and Health, Sydney Medical School, University of Sydney, NSW 2050, Australia.
E-mail: emily.blyth@sydney.edu.au

Received 25 July 2020;
Revised 22 September 2020;
Accepted 29 September 2020

doi: 10.1002/cti2.1200

Clinical & Translational Immunology
2020; **9**: e1200

Abstract

Objective. Adoptive immunotherapy with *ex vivo* expanded tumor-specific T cells has potential as anticancer therapy. Preferentially expressed antigen in melanoma (PRAME) is an attractive target overexpressed in several cancers including melanoma and acute myeloid leukaemia (AML), with low expression in normal tissue outside the gonads. We developed a GMP-compliant manufacturing method for PRAME-specific T cells from healthy donors for adoptive immunotherapy. **Methods.** Mononuclear cells were pulsed with PRAME 15-mer overlapping peptide mix. After 16 h, activated cells expressing CD137 were isolated with immunomagnetic beads and cocultured with irradiated $CD137^{neg}$ fraction in medium supplemented with interleukin (IL)-2, IL-7 and IL-15. Cultured T cells were restimulated with antigen-pulsed autologous cells after 10 days. Cellular phenotype and cytokine response following antigen re-exposure were assessed with flow cytometry, enzyme-linked immunospot (ELISPOT) and supernatant cytokine detection. Detailed phenotypic and functional analysis with mass cytometry and T-cell receptor (TCR) beta clonality studies were performed on selected cultures. **Results.** PRAME-stimulated cultures (n = 10) had mean expansion of 2500-fold at day 18. Mean $CD3^{+}$ percentage was 96% with CD4: CD8 ratio of 4:1. Re-exposure to PRAME peptide mixture showed enrichment of CD4 cells expressing interferon (IFN)-γ (mean: 12.2%) and TNF-α (mean: 19.7%). Central and effector memory cells were 23% and 72%, respectively, with 24% T cells expressing PD1. Mass cytometry showed predominance of Th1 phenotype

(CXCR3$^+$/CCR4^{neg}/CCR6^{neg}/Tbet$^+$, mean: 73%) and cytokine production including IL-2, IL-4, IL-8, IL-13 and GM-CSF (2%, 6%, 8%, 4% and 11%, respectively). **Conclusion.** PRAME-specific T cells for adoptive immunotherapy were enriched from healthy donor mononuclear cells. The products were oligoclonal, exhibited Th1 phenotype and produced multiple cytokines.

Keywords: adoptive immunotherapy, antigen-specific T cells, PRAME, preferential expressed antigen in melanoma

INTRODUCTION

Adoptive T-cell therapies are under investigation for the treatment of a variety of malignancies. These include *ex vivo* expanded tumor-infiltrating lymphocytes (TILs),[1,2] *ex vivo* expanded circulating tumor antigen-specific T lymphocytes[3,4] and genetically modified products such as chimeric antigen receptor (CAR)[5,6] and transgenic T-cell receptor (TCR)-modified T cells.[7,8] Naturally occurring T cells that recognise intracellular or extracellular tumor-associated antigens or neoantigens formed by malignant genetic alterations can be *ex vivo* expanded and used therapeutically.[9] There are a number of small trials of this approach.[10–13]T cells reactive against BCR-ABL[14], PML-RARa[15], proteinase 3[16] and WT1[9] can be isolated and demonstrate specific cytolytic activity *in vitro*.[4,16,17] Identification of potential antigen targets is underway in many malignancies.[18,19]

Preferential antigen in melanoma (PRAME) is overexpressed in a wide variety of tumor types including AML,[20] melanoma,[21] renal cell carcinoma,[22] acute lymphoblastic leukaemia,[23] chronic myeloid leukaemia,[24] Hodgkin lymphoma[25] and medulloblastoma.[26] Moreover, its low expression in normal healthy tissue apart from gonadal tissue[20] makes it an attractive target for cellular immunotherapy.

To date, methods of *ex vivo* expansion of TAA-specific T cells rely on the use of antigen-presenting cells (APCs) such as dendritic cells or engineered artificial antigen-presenting cells.[9,27–29] This approach is labour-intensive, time-consuming, associated with higher cost and may be difficult to translate to GMP-compliant processes for clinical use. To address this, we developed a protocol for immunomagnetic bead selection of T cells expressing the activation marker CD137 (4-1BB) after exposure to overlapping PRAME peptides as a rapid method of *ex vivo* expansion for clinical use (Figure 1). CD137 is a costimulatory molecule and a member of the tumor necrosis factor receptor (TNFR) family. Transient increased expression is seen on cells that have been activated by TCR engagement and signalling.[30] We utilised this feature to select and expand PRAME-specific T cells and performed phenotypic and functional analysis of the final cell product. The method we describe is robust using mononuclear cells from healthy donors and readily applicable to clinical use. A clinical trial utilising this protocol to prevent postallogeneic haemopoietic stem cell transplant relapse has been initiated (ANZ CTR NCT02895412).

RESULTS

Determining maximal CD137 expression

In order to determine the optimum time for CD137$^+$ cell selection, a time course was performed to determine the expression at 0, 16, 24 and 41 h after antigen challenge. Maximal cell surface CD137 expression by flow cytometry was achieved 16–24 h after previously expanded antigen-specific T cells were rechallenged with antigen-derived peptide mixture and anti-CD28 antibody (Figure 2).

CD137$^+$-activated T-cell isolation and expansion

The mean percentage of CD137$^+$-enriched cells isolated by immunomagnetic bead separation from PBMC was 0.6% of total starting cells (range 0.04–1.72%). There was no significant difference between the steady state or G-MNC starting material (mean 0.9% and 0.36%, respectively, $P = 0.093$; Figure 3a). In the CD137-enriched fraction, the proportion of CD3$^+$ cells which expressed CD137$^+$ by fluorescence flow cytometry was 67% (range 13–89.1%) with no significant

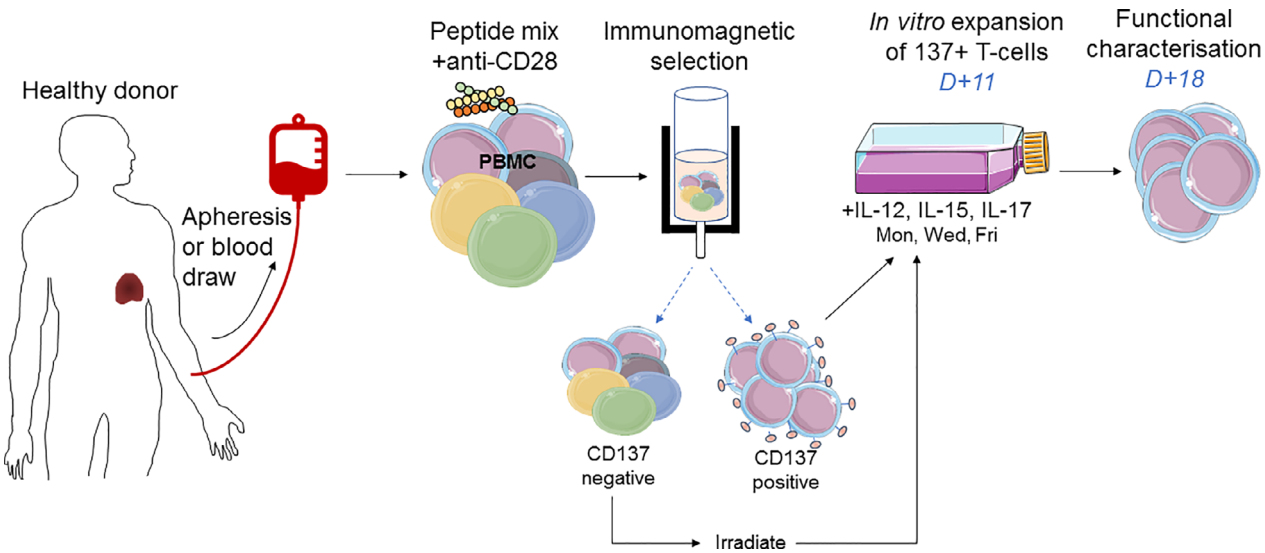

Figure 1. Method for *ex vivo* expansion of CD137-expressing activated T cells.

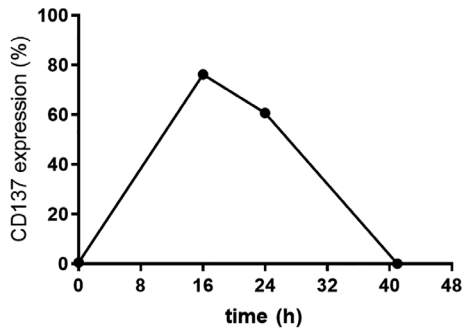

Figure 2. CD137 expression is maximal at 18–24 h following exposure to PRAME peptide mixture. CD137 expression by cultured T cells following re-exposure to PRAME peptide mixture measured by flow cytometry at 16, 24 and 41 h. (n = 1).

difference between the different starting material (means of 62.7% and 70.6% for PBMC and G-MNC, respectively, P = 0.60; Figure 3b). Using PBMC as starting material, the cell expansion by the end of culture was 148-fold (range 96–210-fold) at 11 days and 2539-fold (range 990–4687-fold) at 18 days. With G-MNC as starting material, expansion after 11 days was 194-fold (range 110–322-fold) and 2138-fold (range 660–5418-fold) after 18 days (Figure 3c). There was no significant difference in expansion kinetics regardless of starting material of PBMC or G-MNC (P = 0.917).

Phenotype by fluorescence cytometry

Immunophenotype of resting cells at the end of culture was measured by fluorescence flow cytometry. The majority of cells were $CD3^+$ T cells (mean 96%, range 92.4–99.6%). CD4 T cells dominated (80% of $CD3^+$, range 55.1–99%; Figure 4). The majority of T cells in culture were $CD45RA^-$ $CD62L^-$ effector memory cells (72%, range 36.4–92.3%). A large population of $CD45RA^-$ $CD62L^+$ central memory cells (23%, range 3.5–59.5%) was also present. The expression of the co-inhibitory marker PD1 was 24.4% (range 3.3–83.5%) with variable expression of Tim3 (range 51.3% (range 13.9–77.2%) and LAG3 (83.5%, range 62.8–95%). More detailed phenotype of the antigen-specific T cells was explored with mass cytometry, described below.

Specificity

Specificity of the cultured T cells was demonstrated by measuring the cytokine production when re-exposed to PRAME-derived peptide mixture using fluorescent flow cytometry, ELISPOT, cytokine detection in culture supernatant and high-dimensional mass cytometry.

Intracellular flow cytometry showed that upon re-exposure to PRAME peptide mixture, compared with media-only control, $CD4^+$ T cells in all cultures secreted significantly more IFN-γ and TNF-α and there was a significant increase in the surrogate degranulation marker CD107 (IFN-γ: mean 12.2% (range 0.2–36.3%) vs 0.5% (0.1–2.3%), P = 0.02; TNF-α: mean 19.7% (1.7–54.6%) vs 0.7% (0.3–1.7%), P = 0.007; CD107: mean 16.6%

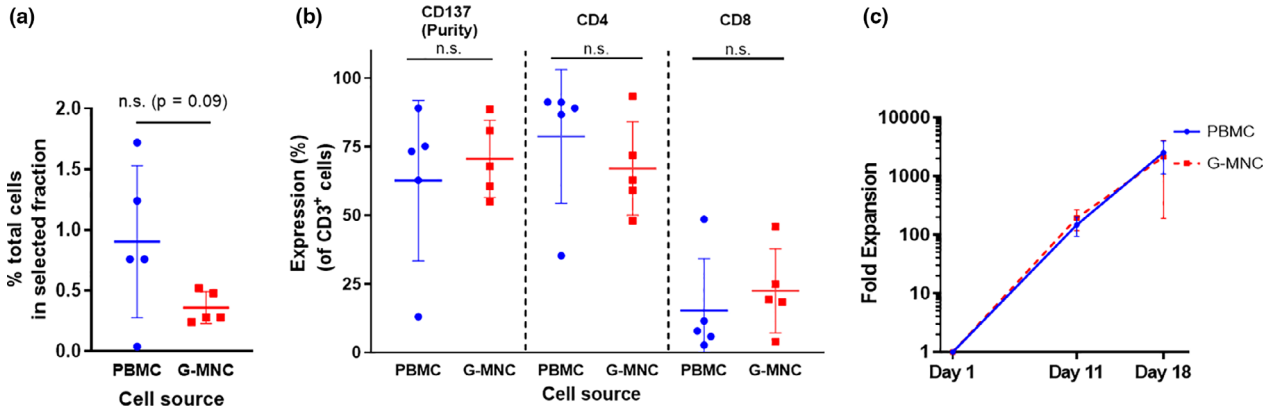

Figure 3. Isolation and expansion of CD137-expressing cells from PBMC. **(a)** Immunomagnetic column CD137 selection yielded a positive fraction ranging from 0.04 to 1.72% of starting cell number with no significant difference between starting material PBMC or G-MNC (n = 5). **(b)** Flow cytometry assessment of CD137 immunomagnetic column selected fraction showing proportions of CD3-positive cell expressing CD137 (n = 5). The majority of these cells are $CD4^+$ T cells. **(c)** *Ex vivo* expansion of cells in culture. Mean expansion of 170-fold and 2500-fold on days 11 and 18, respectively. G-MNC, G-CSF-primed apheresis-derived mononuclear cells; PBMC, peripheral blood mononuclear cells; G-MNC G-CSF-stimulated mononuclear cells.

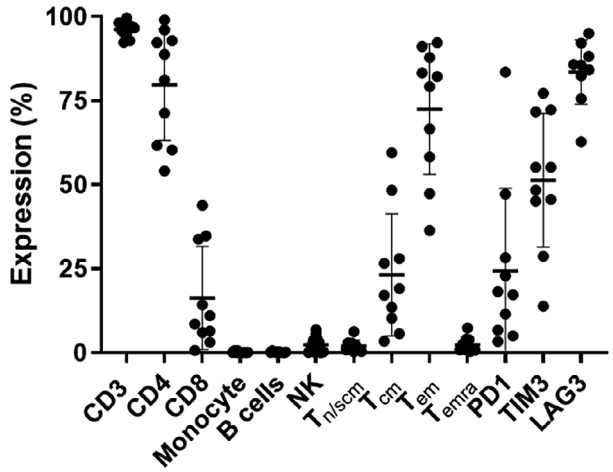

Figure 4. Fluorescence flow cytometry on PRAME-specific T-cell cultures (n = 10). At the end of culture, the majority of cells were $CD3^+$ T cells with preponderance for $CD4^+$ helper T cells. $CD14^+$ monocytes, $CD19^+$ B cells and $CD3^{neg}CD56^+$ NK cells were virtually absent. There was predominance of $CD45RA^{neg}CD62L^+$ central memory T cells and $CD45RA^{neg}CD62L^{neg}$ effector memory T cells. There is variable expression of co-inhibitory markers PD1, Tim3 and LAG3 above isotype control.

(0.7–48.8%) vs 1.4% (0.3%–2.4%), P = 0.01). There was also increased expression of CD107 by $CD8^+$ T cells (mean 12.9% (0.1–43.7%) vs 2.2% (0.2–8.0%), P = 0.04). $CD8^+$ PRAME antigen-specific IFN-γ and TNF-α responses were seen in 5 of 10 cultures (the proportion of responsive $CD8^+$ T cells in these 5 cultures: IFN-γ mean 13.6%, range 3.6–33.3%; TNF-α mean 12.7%, range 2.3–33%). However, in all cultures, there was not a statistically significant difference in PRAME-specific $CD8^+$ IFN-γ^+ and TNF-α^+ compared with unstimulated cells at the end of culture (IFN-γ mean 7.1% (0.1–33.3%) vs 0.9% (0.1–3.0%), P = 0.09; TNF-α mean 6.7% (0.3–33%) vs 0.4% (0.0–1.1%), P = 0.10; Figure 5a).

A response to PRAME was demonstrated by ELISPOT with a mean of 981 SFU/10^5 cells (range 37–2678 SFU/10^5 cells) compared with 25 SFU/10^5 cells (range 16–32 SFU/10^5 cells) in the negative control and 27 SFU/10^5 cells (13–42 SFU/10^5 cells) when exposed to irrelevant peptide mixture (WT1) (Figure 5b and c).

In order to assess the secretion of an extended selection of cytokines, the supernatant of 2 cultures was harvested with or without re-exposure to PRAME-derived peptide mixture and incubated with cytokine array. This showed increased levels of Th1 (IFN-γ, TNF-α, IL-2) as well as Th2 cytokines (IL-4, IL-5, IL-13) (Figure 5d and Supplementary figure 1).

Mass cytometry

Production of cytokines by individual cells was assessed by mass cytometry on three cultures. Choice of antibody targets was based on the results obtained from the cytokine array. tSNE was used to visualise the distribution of cytokine production in individual cells (Figure 6a). Production of TNF-α, IFN-γ, IL-2, IL-4, IL-8, IL-13

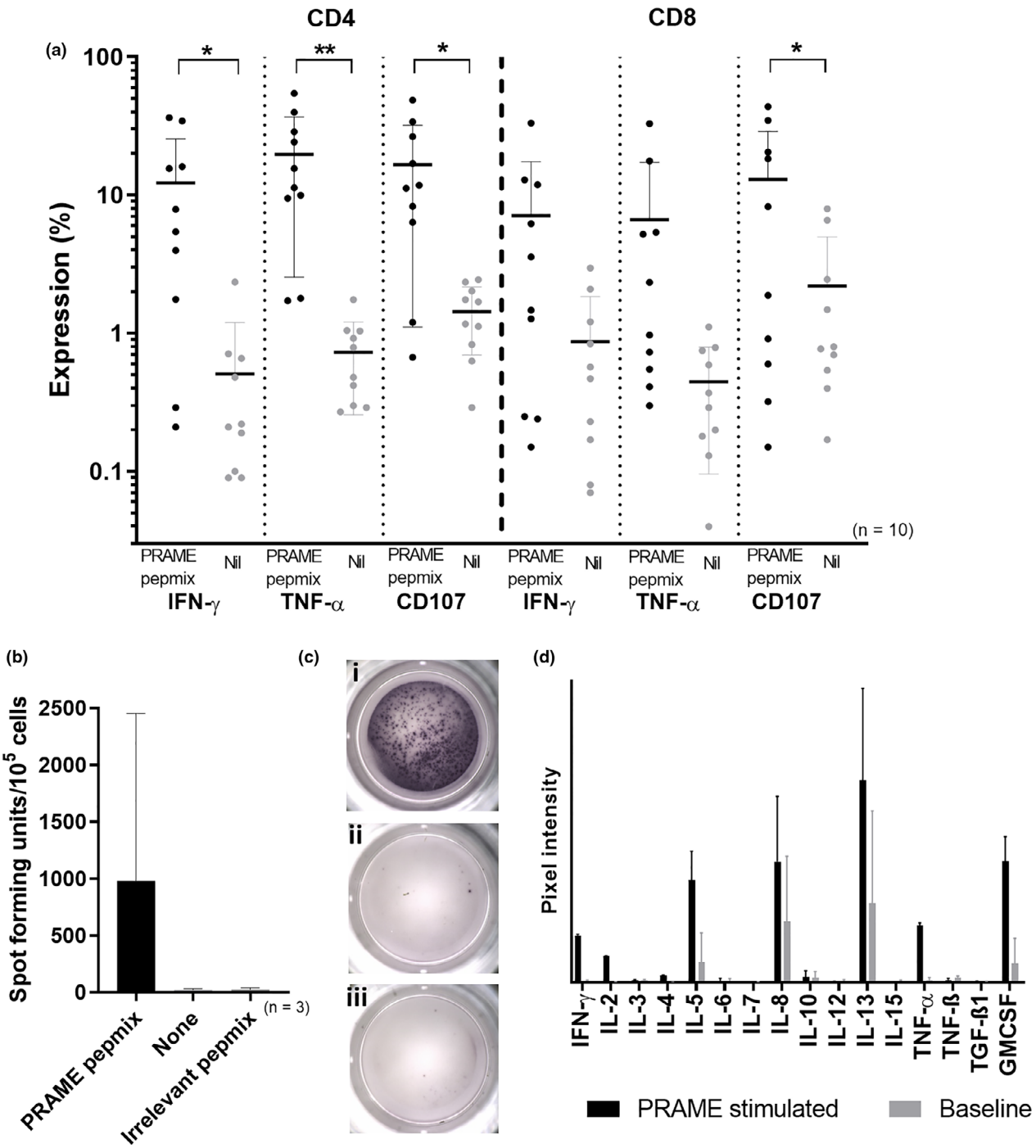

Figure 5. Antigen specificity of the cultured T cells by cytokine release in response to re-exposure to PRAME. **(a)** Expression of IFN-γ and TNF-α and CD107 degranulation in the $CD4^+$ and $CD8^+$ T cells following 18 days of culture in 10 cultures following restimulation to PRAME peptide mixture (PRAME) or no restimulation (Nil). Pooled data represented as mean ± SD. $*P < 0.05$; $**P < 0.01$. ($n = 10$) **(b)** IFN-γ ELISPOT was performed on 3 PRAME-specific T-cell cultures (PRAME peptide mixture vs negative controls media only and irrelevant peptide mixture). **(c)** Photograph of representative wells from Elispot assay with cultured T cells incubated with (i) PRAME peptide mixture; (ii) media only; (iii) irrelevant peptide mixture. **(d)** Supernatant harvested from 2 cultures analysed with cytokine antibody membrane array showed increases in Th1 cytokines (IFN-γ, TNF-α, IL-2) as well as Th2 cytokines (IL-4, IL-5, IL-13).

and GM-CSF in response to re-exposure to PRAME-derived peptide mixture was primarily by $CD4^+$ cells. There was evidence of degranulation with increased expression of CD107. The responding cells corresponded numerically with those identified as antigen responsive in fluorescence flow cytometry. $CD4^+$ T cells were further characterised by sequential gating[31] (Figure 6b), with the majority of $CD4^+$ T cells showing Th1 or Th17 phenotype ($CXCR3^+$) (mean 73%, range 59.6–87.5%) with Th2 cells ($CXCR3^{neg}CCR4^+CCR6^{neg}$) comprising 8% (2.9–13.1%) of $CD4^+$ T cells (Figure 6b).

The $CD4^+$ population secreting multiple cytokines in response to PRAME was gated as shown in Figure 6c for further analysis. The threshold for positivity of the cytokines and degranulation markers is determined based on the unstimulated sample (Figure 6d). The cytokine producing populations from the three cultures had similar extended phenotype as shown in Figure 6e with CD3, 4, 8, memory phenotypes and co-inhibitory markers PD1, Tim3 and LAG3 correlating numerically with fluorescence flow cytometry. The activation marker CD154 was increased more than CD137 at 4 hours after re-exposure to the peptide mixture. The cells were transcriptionally active with high expression of Tbet expression supporting Th1 phenotype. GATA3 (transcription regulator for Th2) showed relatively modest increase in expression. Eomes, the CD8 transcription regulator, was unexpectedly elevated in these $CD4^+$ cells. FoxP3 was highly expressed with negligible IL-10 expression.

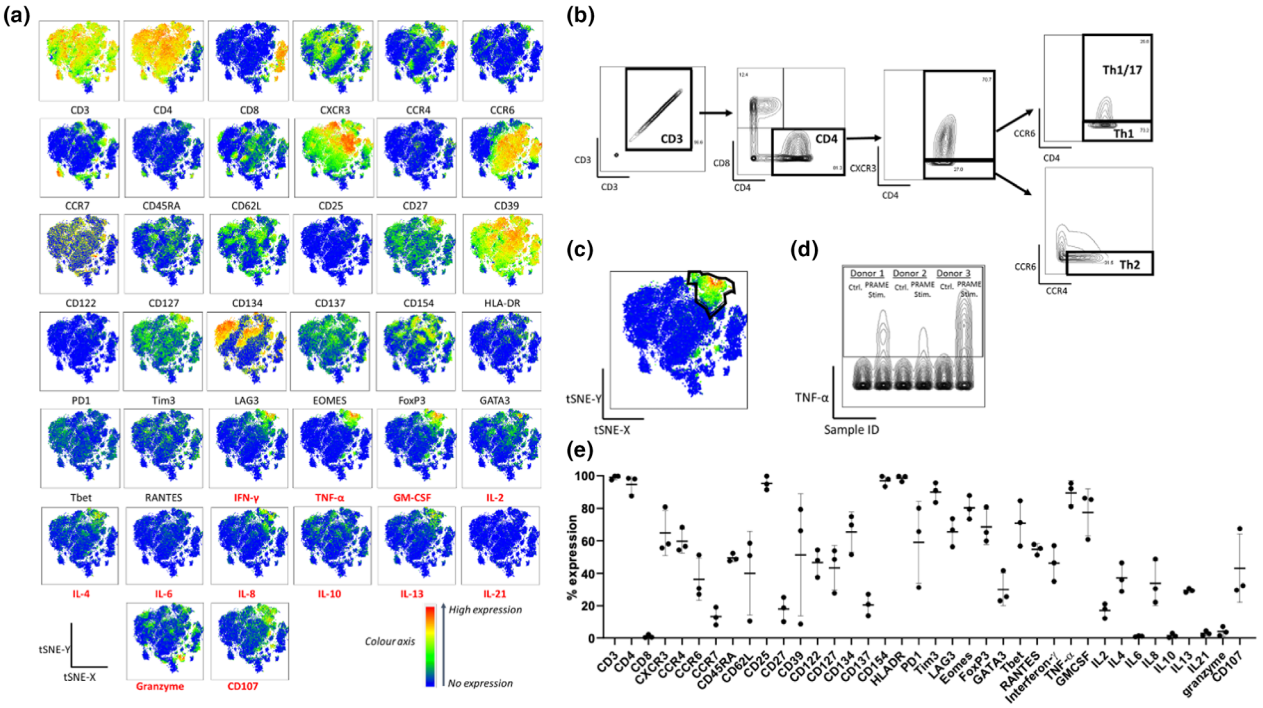

Figure 6. Extended phenotype and cytokine production assessed by mass cytometry. **(a)** Mass cytometry was performed on three cultures after stimulation with PRAME-derived peptide mix and analysed with *t*SNE dimensionality reduction with algorithm-based clustering of cells deemed immunophenotypically similar on the 38 selected parameters as detailed in the Methods section. Dots on each tSNE plot in the same position represent the same cell. The expression of various markers is coded by the colour gradient with warmer colours correlating to higher expression. **(b)** Sequential gating on mass cytometry demonstrated predominance of Th1 helper phenotype with 51.9% (range 46.3–61.6%) of $CD4^+$ T cells displaying a Th1 phenotype as defined by $CXCR3^+CCR6^{neg}$ and a further 20.7% (12.8–25.5%) with Th1/Th17 phenotype $CXCR3^+CCR6^+$. 7.5% (2.7–12.3%) of $CD4^+$ T cells had $CXCR3^{neg}CCR4^+CCR6^{neg}$ Th2 phenotype. **(c)** Cytokine-releasing cells (16.1%, range 8.8–35.7%) were gated for further analysis on tSNE plots. **(d)** Threshold for positivity of individual parameters was determined based on signal separation in contour plots with the exception of cytokines (IFN-γ, TNF-α, GM-SCF, IL-2, IL-4, IL-6, IL-8, IL-10, IL-13, IL-21) and degranulation markers (granzyme and CD107) where the thresholds were set with unstimulated specimens (representative example of TNF-α shown). **(e)** Extended phenotypic expression of each parameter of the cytokine secreting subset of cells on mass cytometry as a proportion of viable cells.

TCR sequencing

In order to assess the clonality of the final product, reactive cells were sorted by the expression of CD137 after restimulation at day 18 of *ex vivo* expansion in 4 cases. After RNA extraction, the CDR3 of the beta TCR of the CD137-positive fraction was sequenced. All *ex vivo* expanded PRAME-specific cell products were oligoclonal (Figure 7). In 3 of 4 cases, the majority of cells in the product were represented by the top 10 clones (mean 59% of clonal repertoire, range 27–73%). The $CD4^+$ and $CD8^+$ T-cell fractions were separately sequenced for case 4 and both fractions showed oligoclonality of TCR expressed.

DISCUSSION

CD137 is a costimulatory receptor belonging to the TNF receptor superfamily and is almost uniformly expressed by activated $CD4^+$ and $CD8^+$ T cells as well as some APCs.[32] The inducible expression of CD137 in T cells upon activation has recently been used as a positive selection marker for immunomagnetic column selection for *ex vivo* expansion of antigen-specific T cells.[33,34] The time to maximal CD137 expression on T cells following exposure to immunogen has been reported to vary from 12 h to 5 days depending on the nature of stimulation.[32,35,36] We found that the maximal CD137 expression using PRAME-derived peptide mixture and CD28 antibody costimulation was at 16–24 h (Figure 2). A small number of CD137-positive T cells were isolated following overnight incubation with PRAME peptide mixture and CD28 antibody. This is not unexpected because of the low frequency of TAA-specific T cells as is consistent with published findings.[34,37] Enrichment and numeric expansion of these cells can be achieved in culture with T-cell medium, supported by cytokines IL-2, IL-7 and IL-15 and feeder cells in the form of irradiated autologous PBMCs or G-MNCs.

There was predominance of $CD4^+$ T cells in the majority of cultures, which is consistent with previous reports.[38,39] Other reports of *in vitro* expanded CD8-dominant PRAME-specific T-cell cultures have utilised substantially different methodology.[9,40] $CD4^+$ T cells have been shown to be an important component of the antitumor T-cell response[41,42] in their role of both activating cytolytic T cells[43] and inducing cytotoxicity independently of $CD8^+$ T cells.[44] Mass cytometry and cytokine array data show that the majority of the $CD4^+$ T cells show characteristics of Th1 function which is associated with *in vivo* efficacy following adoptive transfer.[42] The majority of the cultured cells have a central or effector memory phenotype, again consistent with previous reports.[34] We and others have previously highlighted the importance of T cells from these memory compartments in long-term persistence of adoptive antigen-specific T cells *in vivo*,[45–47] and which may be associated with superior clinical outcome.[48,49] There is modest expression of co-inhibitory receptors PD-1, Tim3 and LAG3, which has been reported to be expressed in activated CD4 T cells with Th1 function.[50] The active proliferation and cytokine response to re-exposure to PRAME pepmix suggest these markers represent a response to antigen stimulation rather than a marker of exhaustion.

The specificity of cultured T cells has been demonstrated using multiple modalities. Given the low precursor frequency of tumor antigen-specific T cells, the proportion of T cells with demonstrable specific response to PRAME peptide mixture represent significant enrichment of specific T cells. Flow cytometry and mass cytometry confirmed a subset of cultured T cells being able to secrete multiple pro-inflammatory cytokines in response to re-exposure to PRAME-derived peptide mixture. Multifunctional T cells are associated with superior efficacy *in vivo*.[51,52]

TCR sequencing shows the T-cell products to be oligoclonal without significant overlap of the clones between donors. This suggests that the original number of clones in the starting material is low and is consistent with other reports of tumor antigen-specific T-cell precursor frequency.[11,37] Further work will include defining the epitope targets and HLA restriction of these products but this is beyond the scope of this manuscript.

This method has the major advantage of requiring no specialised antigen-presenting cells such as dendritic cells.[47,53–55] Instead, we relied on the antigen-presenting capacity of monocytes and other APCs in isolated PBMCs or G-MNC to present the oligopeptides with anti-CD28 antibody providing costimulation. This results in reduced personnel time required for manipulation of cells and shorten overall manufacturing timeframe. The use of scanning oligopeptide peptide mixture allows *ex vivo* expansion of T

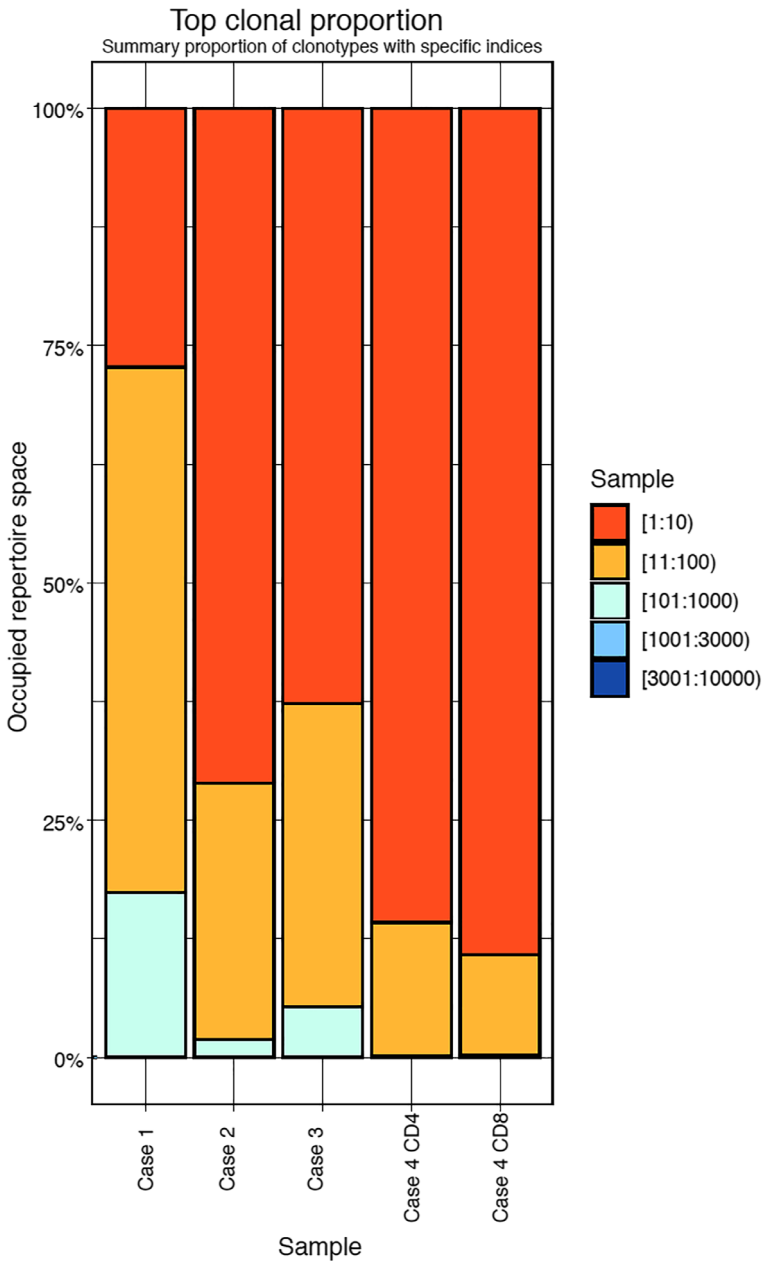

Figure 7. TCR sequencing. TCR clonal proportions of each culture depicting the relative repertoire spaces occupied by clones ordered by prevalence as indicated in the legend.

cells without the need to customise oligopeptide sequences based on the major histocompatibility complex (MHC) type of the donor. The source of starting material for T-cell culture did not have any significant effect on the isolation or expansion of PRAME-specific T cells. We have incorporated manufacture of *ex vivo* expanded antigen-specific T cells for clinical use into routine transplant donor assessment processes to improve clinical translation feasibility. This methodology is currently in use in an ongoing phase I clinical trial (NCT02895412) of *ex vivo* expanded donor-derived pathogen-specific and tumor antigen-specific T cells following allogeneic stem cell transplant for patients with acute myeloid leukaemia.

In conclusion, we have developed a method of *ex vivo* expansion of PRAME-specific T cells for clinical use and demonstrated the *in vitro*

antigen specificity of the cultured T cells, which display a Th1 phenotype associated with favorable *in vivo* function and persistence after adoptive transfer.

METHODS

Donors

Healthy donors provided informed consent in accordance with the Declaration of Helsinki following ethics approval from the Sydney West Local Health District Human Research Ethics Committee. T cells for the starting material were derived from peripheral blood mononuclear cells (PBMCs) collected at steady state or from G-CSF-stimulated apheresis products (G-MNC) from healthy allogeneic stem cells donors procured as part of routine transplantation practice. PBMC isolation was performed as previously described by gradient density centrifugation in Ficoll-Hypaque (GE Healthcare, NSW, Australia).[56] For T-cell products generated from apheresis, a small percentage of harvest (approximately 0.5–1%) was taken as starting material if the amount of the harvest was $> 2.5 \times 10^6$ $CD34^+$ cells/kg of recipient bodyweight, as previously described.[53] HLA typing of 4 healthy donors on which TCR sequencing was performed was done commercially by PathWest Laboratory Medicine, Western Australia, using next-generation sequencing, and is shown in Supplementary table 1.

Peptides

PRAME peptide mixture [lyophilised pentadecapeptide mixtures with 11 amino acid overlaps covering the sequence of PRAME (UniProtKB Acc. no. P78395)] was reconstituted as per manufacturer's instructions (Miltenyi Biotec, Bergisch Gladbach, Germany) and frozen in 1 μg/peptide aliquots. WT1 (Swiss-Prot Acc. no. P19544) peptide mixture (Miltenyi Biotec) used as the irrelevant peptide mixture for negative controls in the ELISPOT assay was similarly reconstituted and aliquoted.

Antigen stimulation and activation marker selection

50×10^6 viable PBMC or G-MNC was resuspended in 1 mL of AIM-V (Gibco-BRL, CA, USA) supplemented with 10% human AB serum (Australian Red Cross Lifeblood, Sydney, Australia). PRAME peptide mixture was added to PBMC to a concentration of 1 μg mL^{-1} per peptide, and anti-CD28 antibody (Miltenyi Biotec) was added to a concentration of 1 μg mL^{-1}. The cells were incubated at 37°C at 5% CO_2 for 1 h. The cultures were then incubated in a 6-well plate for a further 16–24 h at concentration of 1×10^7 mL^{-1} by adding medium with CD28 antibody to maintain concentration of 1 μg mL^{-1}. $CD137^+$ cells were labelled with CD137-PE and anti-PE MicroBeads (Miltenyi Biotec) as per manufacturer's instructions. $CD137^+$ cells were isolated by positive selection with MS MACS columns using miniMACS magnetic separators.

Ex vivo expansion

The *ex vivo* expansion method is shown in Figure 1. The $CD137^{neg}$ cells from the flow through of immunomagnetic column selection were irradiated (30 Gy) and cocultured with $CD137^+$ cells at a $CD137^{neg}$:$CD137^+$ ratio of 100:1 at a total cell concentration of 2×10^6 mL^{-1} in AIM-V medium supplemented with 10% human AB serum in G-REX10 bioreactors (Wilson Wolf, MN, USA). Culture medium was supplemented with IL-2, IL-7 and IL-15 (all cytokines from Miltenyi Biotec) every 2–3 days to a final concentration of 20 U mL^{-1}, 200 U mL^{-1} and 200 U mL^{-1}, respectively. Restimulation with PRAME primed autologous irradiated PBMCs was performed after 10 days in culture. Autologous cells were primed for 1 h with PRAME peptide mixture at final concentration of 1 μg mL^{-1} and irradiated (30 Gy) before being added at a ratio of 2:1. The coculture was resuspended in AIM-V at 2×10^6 mL^{-1} with anti-CD28 antibody.

Fluorescence cytometry

Immunophenotyping of cultured cells was performed at the end of culture with antibodies against CD3, CD4, CD8, CD14, CD19, CD56, CD62L, CD45RA, PD1, LAG3, Tim3, CTLA4 (all BD Biosciences, NJ, USA) and the viability marker Fluorogold (Molecular Probes, OR, USA). Antibody clone and fluorochrome conjugation are listed in Supplementary table 2. 1×10^6 cells from each culture were stained in a 100 μL volume with antibody cocktail for 30 min and washed in flow cytometry buffer (phosphate-buffered saline with 0.5% bovine serum albumin and 0.1% sodium azide) before being acquired with FACS Fortessa (BD biosciences) flow cytometer.

For intracellular cytokine staining, 0.5×10^6 cells were incubated with an overlapping peptide mix of PRAME (Miltenyi Biotec) for 5 h in the presence of anti-CD28 (L293) and CD49d (L25) antibodies (BD Biosciences). Monensin (2 μm; BD biosciences) and brefeldin A (1 μg mL^{-1}; BD biosciences) were added for the last 4 h, followed by labelling with fluorochrome-conjugated antibodies against surface antigens CD3, CD4 and CD8 and degranulation marker CD107a + b (H4A3 and H4B4) and viability marker 7-AAD (BD biosciences). Intracellular labelling for IFN-γ (B27) and TNF-α (Mab-11) was performed using the Cytofix/Cytoperm Kit (BD Biosciences) according to the manufacturer's instructions. T cells stimulated with 5 ng mL^{-1} phorbol 12-myristate 13-acetate (PMA) and 1 ng mL^{-1} ionomycin (Sigma-Aldrich, MO, USA) were used as positive controls, and unstimulated cultured T cells were used as negative controls. Samples were acquired with a FACS Canto II (BD Biosciences) flow cytometer and analysed with FlowJo version 10 (Tree Star, Inc., OR, USA).

PRAME-specific T-cell cultures were restimulated with PRAME peptide mixture, and activation marker expressing cells were isolated for T-cell receptor (TCR) sequencing. Sixteen hours after stimulation, cells were resuspended in phosphate-buffered saline containing 5% foetal bovine serum (PBS + 5%FBS) and 20% human FCR blocking reagent (Miltenyi Biotec), stained with CD3, CD4, CD8, CD137, CD154 and viability marker 7-AAD (all BD Biosciences) for 20 min at 4°C and washed and resuspended

in 100 μL PBS + 5% FBS. They were then sorted on a BD FACSAriaIII (BD Biosciences) using a 70-μm nozzle into $CD3^+CD4^+$ or $CD3^+CD8^+$ $CD137^+$ and/or $CD154^+$ populations (gating strategy shown in Supplementary figure 2). In cases with $CD8^+$ T cells < 10%, the $CD4^+$ and $CD8^+$ fractions were not separated.

Mass cytometry

T cells were prepared for mass cytometry by incubating 2×10^6 cells with PRAME peptide mixture for 5 h in the presence of anti-CD28 (L293) and CD49d (L25) antibodies. Monensin (2 μm) and brefeldin A (1 μg mL^{-1}) were added for the last 4 h. Cells were then stained with cisplatin as a DNA identifier followed by heavy metal-conjugated monoclonal antibodies for mass cytometry analysis as previously described.[57] Dimensionality reduction analysis was performed with the t-stochastic neighbourhood embedding (tSNE) algorithm (implemented in FlowJo as a PlugIn). A fixed number of 7000 cells per condition was sampled at random without replacement from each file and combined for analysis. The markers used for clustering were CD3, CD4, CD8, CXCR3, CCR4, CCR6, CCR7, CD45RA, CD62L, CD25, CD27, CD39, CD122, CD127, CD134, CD154, PD1, Tim3, LAG3, HLA-DR, IL-2, IL-4, IL-6, IL-8, IL-10, IL-13, IL-21, GM-CSF, IFN-γ, TNF-α, CD107, granzyme, RANTES, GATA3, Eomes, FoxP3, Tbet. Antibody clone and heavy metal conjugation are listed in Supplementary table 3.

ELISPOT

IFN-γ enzyme-linked immunospot assay (ELISPOT) was performed on cells at the end of culture using a previously described method modified for PRAME antigen.[32] Briefly, $0.5–2 \times 10^5$ cells were suspended in 200 μL of AIM-V/10% human AB serum and stimulated with PRAME peptide mixture for 18 h in 96-well filter plates (MAIPS4510; Millipore) coated with capture antibody (51-2555KZ; BD Biosciences). Following wash and incubation with detection antibody (51-1890KZ; BD Biosciences), immunospots were developed using ExtrAvidin and SigmaFast BCIP/NBT alkaline phosphatase substrate (Sigma-Aldrich, St Louis, MO) in accordance with manufacturer's directions. The plates were analysed with the AID ELISPOT Reader (Autoimmune Diagnostika, Strassberg, Germany). Tests were performed in triplicates and spots were counted manually.

Cytokine array

PRAME-specific T cells were incubated with PRAME peptide mixture for 5 h in the presence of anti-CD28 (L293) and CD49d (L25) antibodies. The supernatant was harvested for the detection of cytokine using dot blot cytokine antibody membrane array (Abcam ab133997, Cambridge, UK) as per manufacturer's instructions; supernatant from end of culture T cells without restimulation was used as a control. The resultant array images were captured with Chemidoc Touch imaging system (Bio-Rad, CA, USA) and analysed with Imagelab v5.2.1 (Bio-Rad) and ImageJ (NIH).

TCR sequencing

TCR sequence acquisition was performed as previously described.[58] RNA was isolated using Qiagen RNeasy Mini kits (Quantitect RT, QIAgen, Hilden, Germany). Using 5 μL of cDNA template per reaction, TCRβ transcripts were PCR-amplified from the *ex vivo* expanded T-cell product using high-fidelity Q5 polymerase (New England Biolabs, MA, USA) and a mix of 19 Trbv-specific forward primers and a single Trbc-specific reverse primer. Forward and reverse primers had distinct 5′ overhang adapter sequences that enabled addition of sample-specific indices and P5/P7 sequencing adapters in a second PCR using the Illumina Nextera XT DNA library preparation kit. Before the second PCR, magnetic beads (Agencourt AMPure XP, Beckman Coulter, CA, USA) were used to enrich amplicons > 100 bp. After determining amplicon concentrations using a QIAxcel capillary electrophoresis machine (Qiagen), equimolar amounts of amplicons from up to 270 samples were pooled into a single tube, concentrated using magnetic beads (Agencourt AMPure XP, Beckman Coulter) and then 300- to 500-bp amplicons were gel-purified before sequencing on an Illumina NextSeq machine, with a short read 1 of 6 bases followed by a read 2 of 145 bases.

Raw sequence fastq files were analysed with FastQC to quality check average base pair scores. Migec checkout function was used to demultiplex and collapse reads into their 10bp Unique Molecular Identifier groups (UMI) using the -cute function to compress output, alter FastQ header with UMI info, adapter trimming and remove trails of template-switching. Mixcr was used to assemble and align reads and to extract Cdr3 sequences. Align function aligned the input demultiplexed reads to the V, D and J T-cell receptor reference sequences with –report option for alignment statistics. Assemble function built the clonotypes using the alignments generated from the align function and according to specific gene features, that is CDR3. Finally, the export function was used to extract the clonotypes, but with the assemble function, with information such as clonotype nucleotide sequence and count to parsable text files for downstream analysis.

Statistical analysis

Statistical analysis was performed using GraphPad Prism version 7.02 (GraphPad, La Jolla, CA, USA). Results are expressed as mean (range minimum–maximum) unless otherwise specified. For comparison of cell expansion parameters and phenotype between the different starting materials, the two-tailed Student's *t*-test was used for comparison between 2 groups. A paired *t*-test was used for comparison of measured parameters between PRAME-stimulated and media-only conditions for experiments determining the specificities of the products (intracellular cytokine flow cytometry, cytokine array and ELISPOT) and for comparison of proportion of cells expressing measured parameters between cytokine secreting subset and noncytokine secreting subset as determined by mass cytometry.

ACKNOWLEDGMENTS

KL is a doctoral candidate at The University of Sydney and has received funding from the Haematology Society of Australia and New Zealand and Sydney West Translational Cancer Research Centre. EB is an NSW Cancer Institute Post-doctoral Fellow. HMM is currently supported by the International Society for the Advancement of Cytometry (ISAC) Marylou Ingram Scholars Program and was previously an NHMRC postdoctoral fellow (GNT1037298). Flow cytometry was performed in the Flow Cytometry Core Facility, which is supported by the Westmead Research Hub, the Cancer Institute of New South Wales and the National Health and Medical Research Council.

CONFLICT OF INTEREST

EB reports advisory board membership Abbvie, Novartis, Astellas and MSD. DG reports advisory Board membership Abbvie, Gilead, Indee Labs and Novartis. KM reports advisory board membership Indee Labs. DG and KM report research funding from Haemalogix. EB, DG, KM and LC report patents in the field of adoptive cell therapy manufacture.

AUTHOR CONTRIBUTIONS

Koon Hiang Lee: Data curation; Formal analysis; Investigation; Methodology; Writing-original draft; Writing-review & editing. **Kavitha Gowrishankar:** Investigation; Project administration; Resources; Supervision; Writing-review & editing. **Janine Street:** Investigation; Methodology. **Helen McGuire:** Formal analysis; Investigation; Methodology; Resources. **Fabio Luciani:** Formal analysis; Resources; Software; Supervision. **Brendan Hughes:** Data curation; Formal analysis; Investigation; Software; Visualization. **Mandeep Singh:** Formal analysis; Investigation; Methodology. **Leighton Clancy:** Methodology; Resources; Validation; Writing-review & editing. **David Gottlieb:** Resources; Supervision; Writing-review & editing. **Kenneth Micklethwaite:** Resources; Supervision; Writing-review & editing. **Emily Blyth:** Conceptualization; Funding acquisition; Methodology; Resources; Supervision; Visualization; Writing-review & editing.

REFERENCES

1. Rosenberg SA, Packard BS, Aebersold PM *et al*. Use of tumor-infiltrating lymphocytes and interleukin-2 in the immunotherapy of patients with metastatic melanoma. *N Engl J Med* 1988; **319**: 1676–1680.
2. Yannelli JR, Hyatt C, McConnell S *et al*. Growth of tumor-infiltrating lymphocytes from human solid cancers: summary of a 5-year experience. *Int J Cancer* 1996; **65**: 413–421.
3. Gottlieb DJ, Li YC, Lionello I *et al*. Generation of tumour-specific cytotoxic T-cell clones from histocompatibility leucocyte antigen-identical siblings of patients with melanoma. *Br J Cancer* 2006; **95**: 181–188.
4. Ohminami H, Yasukawa M, Fujita S. HLA class I-restricted lysis of leukemia cells by a $CD8^+$ cytotoxic T-lymphocyte clone specific for WT1 peptide. *Blood* 2000; **95**: 286–293.
5. Lee DW, Kochenderfer JN, Stetler-Stevenson M *et al*. T cells expressing CD19 chimeric antigen receptors for acute lymphoblastic leukaemia in children and young adults: a phase 1 dose-escalation trial. *Lancet* 2015; **385**: 517–528.
6. Brentjens RJ, Davila ML, Riviere I *et al*. CD19-targeted T cells rapidly induce molecular remissions in adults with chemotherapy-refractory acute lymphoblastic leukemia. *Sci Transl Med* 2013; **5**: 177ra38.
7. Rapoport AP, Stadtmauer EA, Binder-Scholl GK *et al*. NY-ESO-1-specific TCR-engineered T cells mediate sustained antigen-specific antitumor effects in myeloma. *Nat Med* 2015; **21**: 914–921.
8. Kageyama S, Ikeda H, Miyahara Y *et al*. Adoptive transfer of MAGE-A4 T-cell receptor gene-transduced lymphocytes in patients with recurrent esophageal cancer. *Clin Cancer Res* 2015; **21**: 2268–2277.
9. Weber G, Gerdemann U, Caruana I *et al*. Generation of multi-leukemia antigen-specific T cells to enhance the graft-versus-leukemia effect after allogeneic stem cell transplant. *Leukemia* 2013; **27**: 1538–1547.
10. Gerdemann U, Katari U, Christin AS *et al*. Cytotoxic T lymphocytes simultaneously targeting multiple tumor-associated antigens to treat EBV negative lymphoma. *Mol Ther* 2011; **19**: 2258–2268.
11. Chapuis AG, Ragnarsson GB, Nguyen HN *et al*. Transferred WT1-reactive $CD8^+$ T cells can mediate antileukemic activity and persist in post-transplant patients. *Sci Transl Med* 2013; **5**: 174ra27.
12. Chapuis AG, Thompson JA, Margolin KA *et al*. Transferred melanoma-specific $CD8^+$ T cells persist, mediate tumor regression, and acquire central memory phenotype. *Proc Natl Acad Sci USA* 2012; **109**: 4592–4594.
13. Hunder NN, Wallen H, Cao J *et al*. Treatment of metastatic melanoma with autologous $CD4^+$ T cells against NY-ESO-1. *N Engl J Med* 2008; **358**: 2698–2703.
14. Bocchia M, Korontsvit T, Xu Q *et al*. Specific human cellular immunity to bcr-abl oncogene-derived peptides. *Blood* 1996; **87**: 3587–3592.
15. Gambacorti-Passerini C, Grignani F, Arienti F, Pandolfi P, Pelicci P, Parmiani G. Human CD4 lymphocytes specifically recognize a peptide representing the fusion region of the hybrid protein pml/RAR alpha present in acute promyelocytic leukemia cells. *Blood* 1993; **81**: 1369–1375.
16. Molldrem J, Dermime S, Parker K *et al*. Targeted T-cell therapy for human leukemia: cytotoxic T lymphocytes specific for a peptide derived from proteinase 3 preferentially lyse human myeloid leukemia cells. *Blood* 1996; **88**: 2450–2457.
17. Matsushita M, Ikeda H, Kizaki M *et al*. Quantitative monitoring of the PRAME gene for the detection of minimal residual disease in leukaemia. *Br J Haematol* 2001; **112**: 916–926.
18. Anguille S, Van Tendeloo VF, Berneman ZN. Leukemia-associated antigens and their relevance to the immunotherapy of acute myeloid leukemia. *Leukemia* 2012; **26**: 2186–2196.

19. Goswami M, Hensel N, Smith BD *et al*. Expression of putative targets of immunotherapy in acute myeloid leukemia and healthy tissues. *Leukemia* 2014; **28**: 1167–1170.
20. Greiner J, Ringhoffer M, Taniguchi M *et al*. mRNA expression of leukemia-associated antigens in patients with acute myeloid leukemia for the development of specific immunotherapies. *Int J Cancer* 2004; **108**: 704–711.
21. Ikeda H, Lethe B, Lehmann F *et al*. Characterization of an antigen that is recognized on a melanoma showing partial HLA loss by CTL expressing an NK inhibitory receptor. *Immunity* 1997; **6**: 199–208.
22. Neumann E, Engelsberg A, Decker J *et al*. Heterogeneous expression of the tumor-associated antigens RAGE-1, PRAME, and glycoprotein 75 in human renal cell carcinoma: candidates for T-cell-based immunotherapies? *Cancer Res* 1998; **58**: 4090–4095.
23. Steinbach D, Viehmann S, Zintl F, Gruhn B. PRAME gene expression in childhood acute lymphoblastic leukemia. *Cancer Genet Cytogenet* 2002; **138**: 89–91.
24. Radich JP, Dai H, Mao M *et al*. Gene expression changes associated with progression and response in chronic myeloid leukemia. *Proc Natl Acad Sci USA* 2006; **103**: 2794–2799.
25. Willenbrock K, Kuppers R, Renne C *et al*. Common features and differences in the transcriptome of large cell anaplastic lymphoma and classical Hodgkin's lymphoma. *Haematologica* 2006; **91**: 596–604.
26. Boon K, Edwards JB, Siu IM *et al*. Comparison of medulloblastoma and normal neural transcriptomes identifies a restricted set of activated genes. *Oncogene* 2003; **22**: 7687–7694.
27. Mitchell MS, Darrah D, Yeung D *et al*. Phase I trial of adoptive immunotherapy with cytolytic T lymphocytes immunized against a tyrosinase epitope. *J Clin Oncol* 2002; **20**: 1075–1086.
28. Maus MV, Thomas AK, Leonard DGB *et al*. *Ex vivo* expansion of polyclonal and antigen-specific cytotoxic T lymphocytes by artificial APCs expressing ligands for the T-cell receptor, CD28 and 4–1BB. *Nature Biotechnol* 2002; **20**: 143.
29. Butler MO, Lee JS, Ansen S *et al*. Long-lived antitumor $CD8^+$ lymphocytes for adoptive therapy generated using an artificial antigen-presenting cell. *Clin Cancer Res* 2007; **13**: 1857–1867.
30. Wolfl M, Kuball J, Ho WY *et al*. Activation-induced expression of CD137 permits detection, isolation, and expansion of the full repertoire of $CD8^+$ T cells responding to antigen without requiring knowledge of epitope specificities. *Blood* 2007; **110**: 201–210.
31. Wei Y, Feng J, Hou Z, Wang XM, Yu D. Flow cytometric analysis of circulating follicular helper T (Tfh) and follicular regulatory T (Tfr) populations in human blood. *Methods Mol Biol* 2015; **1291**: 199–207.
32. Wen T, Bukczynski J, Watts TH. 4–1BB ligand-mediated costimulation of human T cells induces CD4 and CD8 T cell expansion, cytokine production, and the development of cytolytic effector function. *J Immunol* 2002; **168**: 4897–4906.
33. Choi BK, Lee SC, Lee MJ *et al*. 4–1BB-based isolation and expansion of $CD8^+$ T cells specific for self-tumor and non-self-tumor antigens for adoptive T-cell therapy. *J Immunother* 2014; **37**: 225–236.
34. Schmied S, Gostick E, Price DA, Abken H, Assenmacher M, Richter A. Analysis of the functional WT1-specific T-cell repertoire in healthy donors reveals a discrepancy between $CD4^+$ and $CD8^+$ memory formation. *Immunology* 2015; **145**: 558–569.
35. Cannons JL, Lau P, Ghumman B *et al*. 4–1BB ligand induces cell division, sustains survival, and enhances effector function of CD4 and CD8 T cells with similar efficacy. *J Immunol* 2001; **167**: 1313–1324.
36. Dawicki W, Watts TH. Expression and function of 4–1BB during CD4 versus CD8 T cell responses *in vivo*. *Eur J Immunol* 2004; **34**: 743–751.
37. Matko S, Odendahl M, Bornhaeuser M, Tonn T. High prevalence of functional Laa specific cytotoxic T lymphocytes in healthy individuals-implications for strategies in adoptive T cell therapies of relapsed leukemia. *Blood* 2015; **126**: 5428.
38. Han S, Huang Y, Liang Y, Ho Y, Wang Y, Chang L-J. Phenotype and functional evaluation of *ex vivo* generated antigen-specific immune effector cells with potential for therapeutic applications. *J Hematol Oncol* 2009; **2**: 34.
39. Gutzmer R, Rivoltini L, Levchenko E *et al*. Safety and immunogenicity of the PRAME cancer immunotherapeutic in metastatic melanoma: results of a phase I dose escalation study. *ESMO open* 2016; **1**: e000068.
40. Quintarelli C, Dotti G, De Angelis B *et al*. Cytotoxic T lymphocytes directed to the preferentially expressed antigen of melanoma (PRAME) target chronic myeloid leukemia. *Blood* 2008; **112**: 1876–1885.
41. Quezada SA, Simpson TR, Peggs KS *et al*. Tumor-reactive $CD4^+$ T cells develop cytotoxic activity and eradicate large established melanoma after transfer into lymphopenic hosts. *J Exp Med* 2010; **207**: 637–650.
42. Muranski P, Restifo NP. Adoptive immunotherapy of cancer using $CD4^+$ T cells. *Curr Opin Immunol* 2009; **21**: 200–208.
43. Keene JA, Forman J. Helper activity is required for the *in vivo* generation of cytotoxic T lymphocytes. *J Exp Med* 1982; **155**: 768–782.
44. Greenberg PD, Kern DE, Cheever MA. Therapy of disseminated murine leukemia with cyclophosphamide and immune Lyt-1^+,2^- T cells. Tumor eradication does not require participation of cytotoxic T cells. *J Exp Med* 1985; **161**: 1122–1134.
45. Berger C, Jensen MC, Lansdorp PM, Gough M, Elliott C, Riddell SR. Adoptive transfer of effector CD8+ T cells derived from central memory cells establishes persistent T cell memory in primates. *J Clin Investig* 2008; **118**: 294–305.
46. Wang X, Wong CW, Urak R *et al*. Comparison of naive and central memory derived $CD8^+$ effector cell engraftment fitness and function following adoptive transfer. *Oncoimmunology* 2016; **5**: e1072671.
47. Withers B, Blyth E, Clancy LE *et al*. Long-term control of recurrent or refractory viral infections after allogeneic HSCT with third-party virus-specific T cells. *Blood Adv* 2017; **1**: 2193–2205.
48. Mueller KT, Maude SL, Porter DL *et al*. Cellular kinetics of CTL019 in relapsed/refractory B-cell acute lymphoblastic leukemia and chronic lymphocytic leukemia. *Blood* 2017; **130**: 2317–2325.

49. Robbins PF, Dudley ME, Wunderlich J *et al*. Cutting edge: persistence of transferred lymphocyte clonotypes correlates with cancer regression in patients receiving cell transfer therapy. *J Immunol* 2004; **173**: 7125–7130.
50. Ozkazanc D, Yoyen-Ermis D, Tavukcuoglu E, Buyukasik Y, Esendagli G. Functional exhaustion of $CD4^+$ T cells induced by co-stimulatory signals from myeloid leukaemia cells. *Immunology* 2016; **149**: 460–471.
51. Ma C, Cheung AF, Chodon T *et al*. Multifunctional T-cell analyses to study response and progression in adoptive cell transfer immunotherapy. *Cancer Discov* 2013; **3**: 418–429.
52. Rossi J, Paczkowski P, Shen YW *et al*. Preinfusion polyfunctional anti-CD19 chimeric antigen receptor T cells are associated with clinical outcomes in NHL. *Blood* 2018; **132**: 804–814.
53. Clancy LE, Blyth E, Simms RM *et al*. Cytomegalovirus-specific cytotoxic T lymphocytes can be efficiently expanded from granulocyte colony-stimulating factor-mobilized hemopoietic progenitor cell products *ex vivo* and safely transferred to stem cell transplantation recipients to facilitate immune reconstitution. *Biol Blood Marrow Transpl* 2013; **19**: 725–734.
54. Blyth E, Clancy L, Simms R *et al*. Donor-derived CMV-specific T cells reduce the requirement for CMV-directed pharmacotherapy after allogeneic stem cell transplantation. *Blood* 2013; **121**: 3745–3758.
55. Blyth E, Gaundar SS, Clancy L *et al*. Clinical-grade varicella zoster virus-specific T cells produced for adoptive immunotherapy in hemopoietic stem cell transplant recipients. *Cytotherapy* 2012; **14**: 724–732.
56. Ramanayake S, Bilmon I, Bishop D *et al*. Low-cost generation of Good Manufacturing Practice-grade CD19-specific chimeric antigen receptor-expressing T cells using piggyBac gene transfer and patient-derived materials. *Cytotherapy* 2015; **17**: 1251–1267.
57. McGuire HM, Shklovskaya E, Edwards J *et al*. Anti-PD-1-induced high-grade hepatitis associated with corticosteroid-resistant T cells: a case report. *Cancer Immunol Immunother* 2018; **67**: 563–573.
58. Wirasinha RC, Singh M, Archer SK *et al*. $\alpha\beta$ T-cell receptors with a central CDR3 cysteine are enriched in $CD8\alpha\alpha$ intraepithelial lymphocytes and their thymic precursors. *Immunol Cell Biol* 2018; **96**: 553–561.

Supporting Information

Additional supporting information may be found online in the Supporting Information section at the end of the article.